

Corrosion resistance in activated fly ash mortars

J.M. Miranda^a, A. Fernández-Jiménez^b, J.A. González^c, A. Palomo^{b,*}

^a*Instituto de Metalurgia (Universidad Autónoma de S. Luis Potosí), México*

^b*Instituto Eduardo Torroja (CSIC), Serrano Galvache s/n, Madrid, 28033, Spain*

^c*CENIM (CSIC), Madrid, Spain*

Received 24 November 2003; accepted 12 July 2004

Abstract

The question of whether reinforcing steel can be protected with activated fly ash cement as effectively as with Portland cement is explored in this study. Corrosion potential (E_{corr}) and polarisation resistance (R_p) values for steel electrodes embedded in Portland cement mortar and two fly ash mortars, respectively activated with NaOH and waterglass+NaOH solutions, are monitored. Chloride-free activated fly ash mortars are found to passivate steel reinforcement as speedily and effectively as Portland cement mortars, giving no cause to fear that corrosion may limit the durability of reinforced concrete structures built with these new types of activated fly ash cement. The polarisation curves and the response to short-term anodic current pulses (galvanostatic pulse technique) obtained further corroborate the full and stable passivation of the steel by the concrete manufactured with these binders.

© 2004 Elsevier Ltd. All rights reserved.

Keywords: Corrosion; Alkali activation; Fly ash

1. Introduction

Portland cement concrete has been the construction material par excellence for decades for its mechanical strength and cost effectiveness, not to mention its properties in general that make it particularly well suited to building. Nonetheless, the destruction of natural quarries entailed in obtaining the prime materials involved, the energy intensity of Portland cement manufacture and the environmental impact of gas emissions (essentially CO₂ and NO_x), etc., have prompted a search for alternative materials. Moreover, the use of conventional concrete is notoriously subject to durability issues, foremost among which are the problems generated by curing at high temperatures (construction during the summer months, thermal treatment during precasting, etc.) or expansive reactions (aggregate–alkali reaction, formation of thaumasite, etc.), etc.

The scientific community is working along several lines of research to provide a solution to all these problems, with the aim of developing alternative binders to replace Portland cement [1–4]. At this time, alkaline cements [5–10] constitute one of the groups with greatest development potential. This new type of cement can be used to manufacture concrete well suited to the precasting industry, because, when thermally cured, it reaches compression strength values of up to 50 or 60 MPa just 20 hours after mixing [11,12]; consequently, the demoulding and storage of precast elements can be expedited, thereby raising factory output. Furthermore, these materials, which adhere extraordinarily well to reinforcing steel, feature high-volume stability, fire resistance and, foreseeably, durability in aggressive environments. Finally, they are competitively priced with respect to Portland cement.

Presumably, given its high alkalinity—even higher than in traditional concrete—and the concomitant positioning of the reinforcing steel in the passivity region on the Pourbaix diagram, alkaline concrete prepared with activated fly ash will guarantee negligible levels of reinforcement corrosion. And although this area has yet to be researched, its

* Corresponding author. Tel.: +34 91 30 20 440; fax: +34 91 30 26 047.
E-mail address: palomo@ietcc.csic.es (A. Palomo).

Table 1
Chemical composition and specific surface of cement and fly ash

	L.o.I. ^a	IR ^b	SiO ₂	Al ₂ O ₃	Fe ₂ O ₃	CaO	MgO	SO ₃	K ₂ O	Na ₂ O	Specific surface (m ² /kg)
CEM I (52.5)	1.48	0.55	19.92	6.44	1.16	63.28	0.63	1.09	–	–	545
Fly ash	1.80	0.40	51.51	27.47	7.23	4.39	1.86	0.15	3.46	0.70	360

^a L.o.I.=Loss on ignition.

^b IR.=Insoluble residue.

importance should not be underestimated because the service life of reinforced concrete structures is often limited by reinforcement corrosion [13–15].

The present paper reports the first experimental data available on the subject, comparing corrosion resistance in a Portland cement mortar to the resistance found in two activated fly ash cement mortars.

2. Experimental

2.1. Materials

The present survey was conducted using a type I commercial Portland cement and a fly ash from a steam power plant in Northern Spain. The chemical analysis of the two materials is given in Table 1, together with the specific surface.

The mortars were prepared with a standardised, evenly graded sand with a quartz content of over 99%.

Finally, the process of activation of the fly ash was approached with aqueous solutions prepared from laboratory grade reagents: NaOH pellets and waterglass with the following percentage composition: 27% of SiO₂, 8.2% of Na₂O and 64.8% of H₂O.

2.2. Procedure

The corrosion potential (E_{corr}) measurements as well as the polarisation resistance (R_p) tests were conducted on small prismatic specimens measuring 8×5.5×2 cm, similar to the ones used in a number of previous studies [16–18]. Two 6-mm diameter steel bars, symmetrically embedded in the prisms, were used as working electrodes during measurement, with a centrally positioned stainless steel wire acting as a counterelectrode. The saturated calomel electrode was the standard reference used in all measurements of electric potential. An active area of 10 cm² was marked on the working electrodes with adhesive tape, thereby isolating the triple steel–mortar atmosphere interface to avoid possible localised corrosion attacks due to differential aeration (Fig. 1). Six different mortars were studied; the respective compositions are given in Table 2.

Mortars 2, 4 and 6 on the one hand, were prepared in the same way as mortars 1, 3 and 5 on the other, except that the former (always even numbers) contained 2% (by binder weight) of Cl[−] in the form of CaCl₂, added during the mixing operation.

The moulds containing the fresh mortar were initially cured at 50 °C in a water-vapour-saturated atmosphere for 20 h, after which the prisms were removed from their respective moulds.

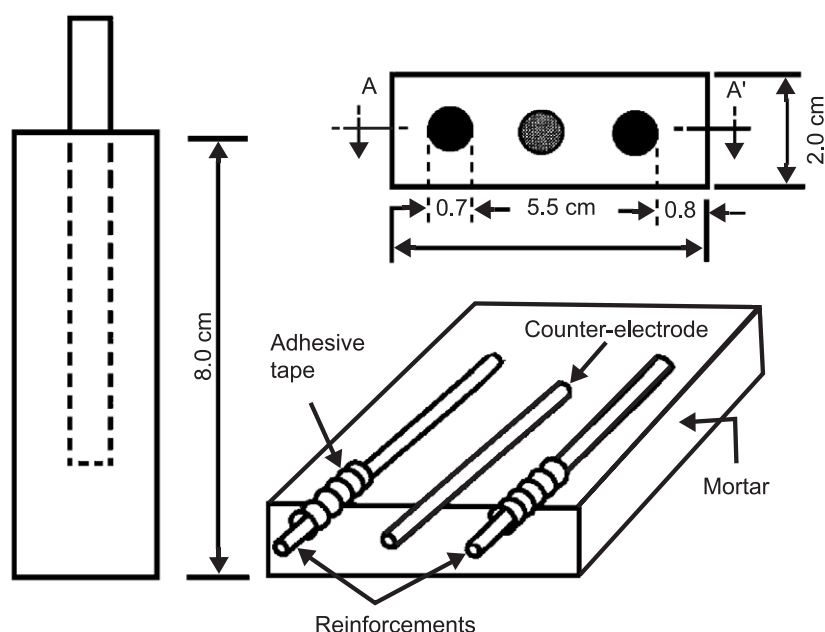


Fig. 1. Prismatic specimens used for the corrosion tests.

Table 2
Mortar composition

Mortar ID Number	Binder	Sand/binder ratio	Dissolution/binder ratio	Type of activating solution
1	Type I cement (52.5)	3/1	0.55	water
2 Cl ⁻	Type I cement (52.5)	3/1	0.55	water
3	Fly ash	2/1	0.35	8 M NaOH
4 Cl ⁻	Fly ash	2/1	0.35	8 M NaOH
5	Fly ash	2/1	0.35	15% waterglass+ 85% (12.5 M NaOH)
6 Cl ⁻	Fly ash	2/1	0.35	15% waterglass+ 85% (12.5 M NaOH)

The activated ash prisms were thermally cured for a further 20 h at 85 °C. Thereafter, a series of prismatic specimens measuring 4×4×16 cm (prepared in parallel with the 8×5.5×2 cm prisms) were compression tested to find the mechanical strength reached by the materials with the curing procedure used, as well as to observe possible microstructural changes generated in the system as a result of activation with different alkali solutions.

After curing at 50 °C, the Portland cement mortar prisms (both the ones intended for mechanical testing and those used in corrosion testing) were kept at room temperature in an atmosphere with high relative humidity (approximately 95%) to further possible deterioration.

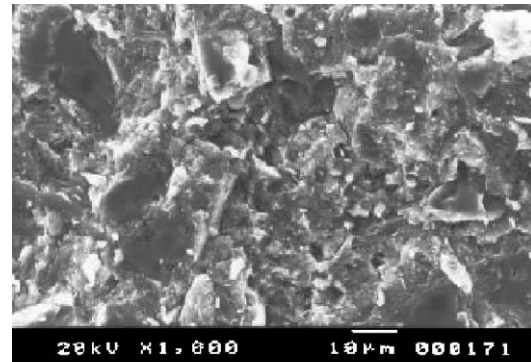
2.3. Measuring techniques

Electrode behaviour over time was monitored with the following: corrosion potential values, E_{corr} ; polarisation resistance values, R_p , to calculate the rate of corrosive attack from the Stern–Geary equation [19]; the shape of the polarisation curves; and the response to galvanostatic pulses. With the exception of E_{corr} , all these procedures provide a quantitative measure of the corrosion rate, a parameter indicative of the corrosion activity or passivity of steel.

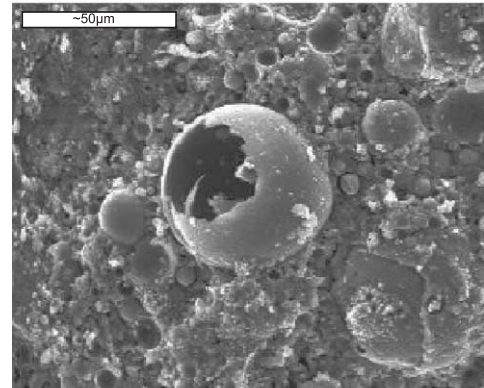
3. Results

The mechanical strengths of the materials studied are given in Table 3. The values at Table 3 were obtained 48 h after the mixing of the mortar components (the binder, the

Micrograph (a) Cement type I (52.5)



Micrograph (b) fly ash + 8M NaOH



Micrograph (c) fly ash + (15%Waterglass + 85% (12.5M NaOH))

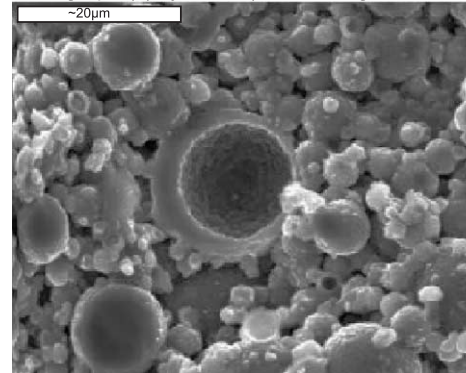


Fig. 2. Microstructural aspect of mortars.

sand, the water, etc.). The curing procedure of these mortar primes was described in the Experimental section. The most interesting aspect to be remarked from Table 3 is that the whole materials investigated have reached a high level of mechanical strength in a relatively short time. Thermal curing has helped a lot to it. Additionally, it should be

Table 3
Mechanical strengths

Samples with Cl ⁻			Samples with Cl ⁻		
Sample	Flexo. (MPa)	Compressive (MPa)	Sample	Flexo. (MPa)	Compressive (MPa)
1 CEM I (52.5)	7.3	38.1	2 Cl ⁻	6.2	43.5
3 Fly ash+ NaOH 8M	5.9	37.4	4 Cl ⁻	6.4	31.0
5 Fly ash+15% waterglass 85% (12.5M NaOH)	10.2	86.32	6 Cl ⁻	12.1	66.0

emphasised the extraordinary effect of waterglass when included in the activating dissolution of fly ashes and also the sensitivity of this type of activating dissolution to the presence of chlorides.

Micrographs (a), (b) and (c) (Fig. 2) in turn, show the most pertinent microstructural aspects of the three working mortars. These pictures reveal the obvious morphological differences between the Portland cement hydrated products (micrograph a) and the products formed as a result of fly ash activation (micrographs b and c). Details explaining the microstructure observed at micrographs b and c can be found at Ref. [22].

Figs. 3a, 4a and 5a show the i_{corr} values, estimated from the R_p measurements taken, respectively, in the Portland cement mortar and the NaOH and “waterglass+ NaOH” activated fly ash mortars, at different specimen ages. The addition of chlorides multiplies the i_{corr} values by a factor of approximately 100 (from 0.01 to 1–10 $\mu\text{A}/\text{cm}^2$). Values of around 1 mA or higher are typical of active corrosion, whereas lower values correspond to passivated steel. Figs. 3b, 4b and 5b illustrate the changes recorded in the E_{corr} values: The findings are very similar for the three mortars in the

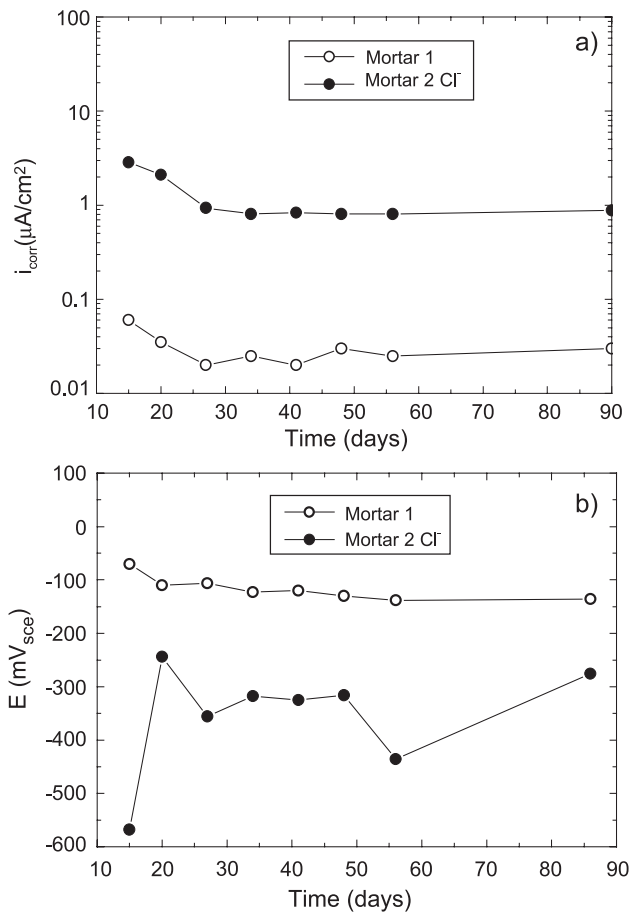


Fig. 3. (a) i_{corr} and (b) E_{corr} values versus time, with steel electrodes symmetrically embedded in the portland cement mortars without and with (2%) of Cl⁻ in relation to the cement weight.

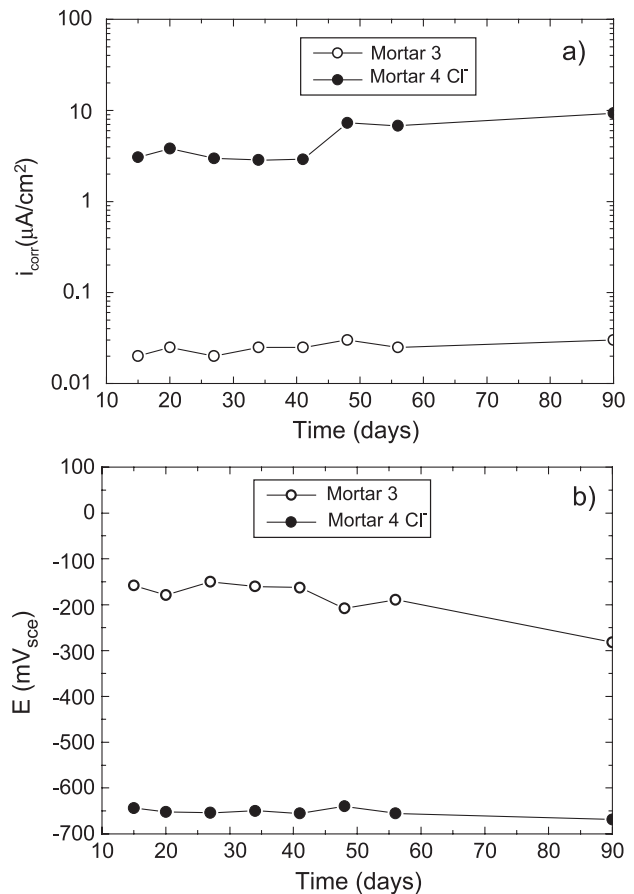


Fig. 4. (a) i_{corr} and (b) E_{corr} values versus time, with steel electrodes symmetrically embedded in the fly ash+8M NaOH mortars without and with (2%) of Cl⁻ in relation to the cement weight.

passive state, ranging from -100 to -200 mV, and substantially more negative for fly ash than for cement mortars when passivation breaks down (around -600 mV compared with -300–400 mV).

Fig. 6a, b and c compares the polarisation curves obtained in the absence and presence of chlorides for the Portland cement and the two activated fly ash mortars, 2 months after the specimens were manufactured. These figures show a substantial difference in current densities—corresponding to the same values of electric potential on the anodic portions of the curves—for mortars with and without chlorides. The responses are similar in the three types of mortar, and current densities are from one to two orders of magnitude higher in chloride-contaminated mortars.

Fig. 7a, b and c represents, also for the three types of mortar, the response to galvanostatic pulses in the presence and absence of chlorides. Visual review of the responses obtained suffices to predict electrode activity or passivity. The chlorides contribute to the rapid attenuation of the polarisation caused by the pulses, with electrodes returning to the levels of electric potential prevailing prior to the test in a matter of seconds or even fractions of a second, whereas in the pulses applied to the electrodes in mortars without

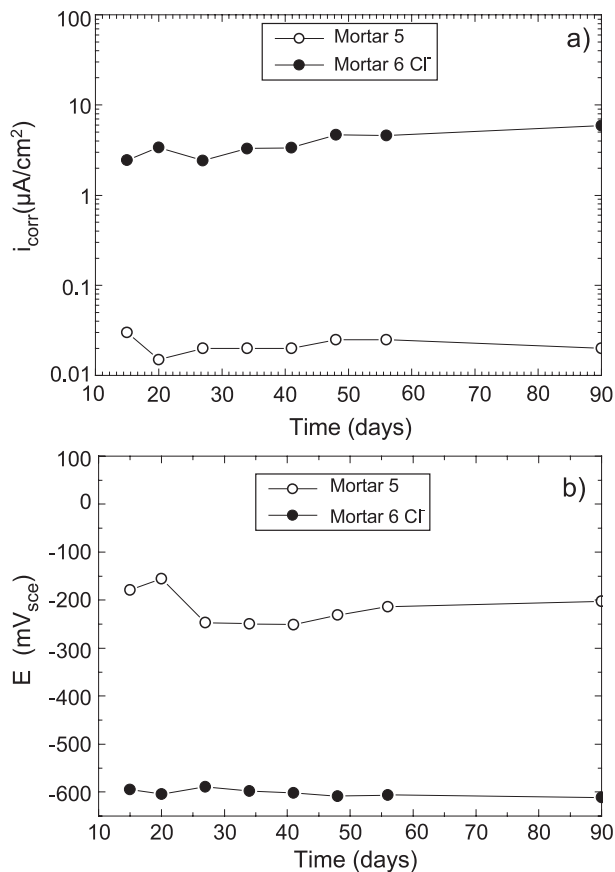


Fig. 5. (a) i_{corr} and (b) E_{corr} values versus time, with steel electrodes symmetrically embedded in the fly ash+(15% waterglass+85% (12.5M NaOH)) mortars without and with (2%) of Cl^- in relation to the cement weight.

chlorides, polarisation is attenuated much more slowly, taking the electrodes several tens of seconds to return to the initial state.

Finally Fig. 8 compares the i_{corr} estimated for all the mortars tested, after 2 months in an atmosphere with very high relative humidity. It should be stressed that in the presence of chlorides, the resulting i_{corr} values are always higher than $1 \mu\text{A}/\text{cm}^2$, whereas the three types of mortar show similar passivating capacities in the absence of chlorides, with values much lower than $0.1 \mu\text{A}/\text{cm}^2$ for the embedded steel electrodes in all cases.

4. Discussion

4.1. Microstructural differences in the working mortars

The microstructural differences between Portland and activated fly ash mortars are readily visible when account is taken of the processes involved in Portland cement hydration and the alkali-activation of fly ash cement. There is a vast amount of information available in the literature on Portland cement, its composition, hydration

mechanisms, technology, etc., whose discussion lies outside the primary aim of the present study; the literature on alkali activation of fly ash, on the contrary, is still very limited.

In this scenario, i.e., with wide differences in the chemical compositions of the CSH gel [20] and the alkaline aluminium silicate generated as a result of fly ash activation [21], the differences in the reaction mechanisms involved in the production of the two types of gel and the kinetic differences in the formation

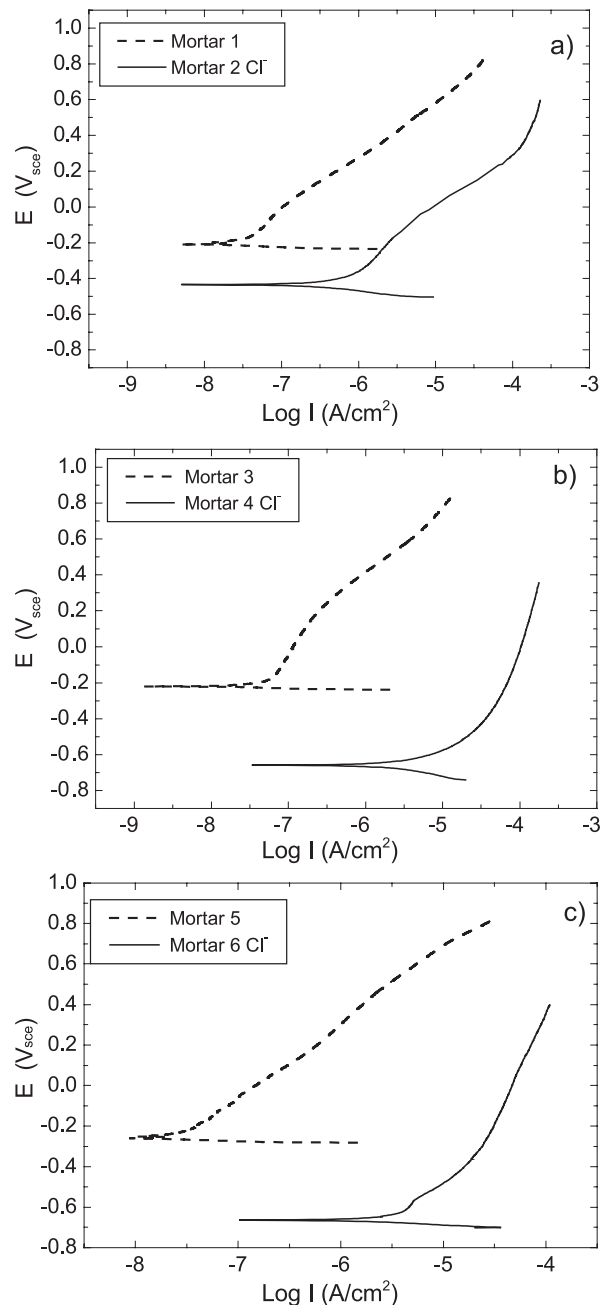


Fig. 6. Polarisation curves of steel embedded in the mortars without and with (2%) of Cl^- in relation to the cement weight: (a) portland cement mortar; (b) fly ash+8M NaOH mortar and (c) fly ash+(15% waterglass+85% (12.5M NaOH)).

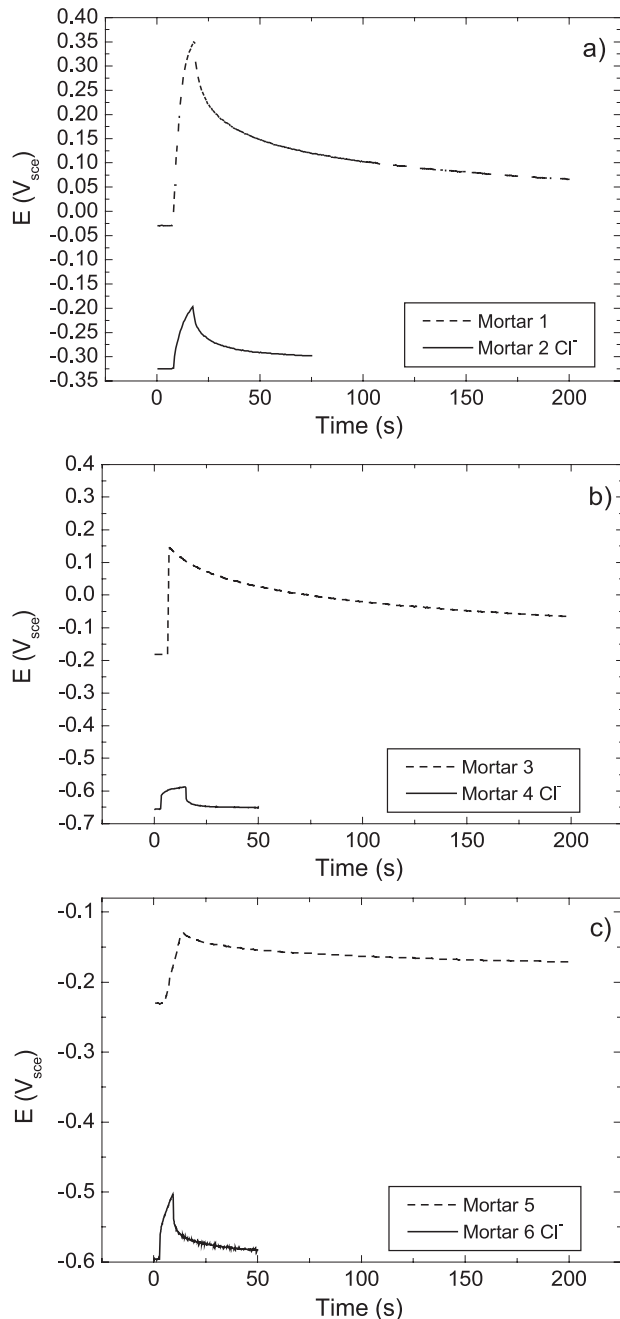


Fig. 7. Relaxation processes of the potential when applying galvanostatic pulses of short duration to the steel electrodes under the same conditions detailed in the previous figure: (a) portland cement mortar; (b) fly ash+8 M NaOH mortar and (c) fly ash+(15% waterglass+85% (12.5M NaOH)).

processes, the protection afforded by the two matrices to embedded reinforcement, should naturally be expected to differ as well.

The mechanical strength values shown in Table 3 and the microstructural elements observed in micrographs (a), (b) and (c) (Fig. 2) confirm not only that the differences mentioned between the three mortars exist, but that they may, at least in part, explain the results described in Figs. 3–8. In this connection, the

following should be stressed with respect to activated fly ash systems:

- The initial pH is very high (higher than in Portland cement systems), although the OH^- groups are absorbed in the cement activation reactions. Moreover, when the amount of reacting material crosses the 45–50% threshold, the kinetics of these reactions plunge to very low levels [21], whereby the system may be expected to store a certain amount of reserve alkalinity over time. In this regard, there are references in the literature to specimens, which, after 5 years of exposure to the elements, retain high alkaline rates due to the absence of carbonation [22], although there are also reports of specimens that are readily carbonated [23]. Curing conditions seem to be crucial to ensuring long-term high alkalinity in the system, which is instrumental to maintain the reinforcing steel in the passivity zone of the Pourbaix “pH potential” diagrams (see Figs. 3a, 4a, 5a and 8).
- Total porosity is slightly lower for waterglass+soda-activated fly ash mortar. The greater impermeability provided by waterglass may retard the diffusion-driven penetration of environmental chlorides and of atmospheric CO_2 . This intriguing possibility has, however, yet to be explored.

4.2. Verification of reinforcing steel corrosion activity or passivity

The following similarities between activated fly ash and Portland cement mortars, from the standpoint of resistance to corrosion, may be deduced from the results in Figs. 3–5:

- The steel is rapidly passivated in systems without chlorides in the three mortars tested, with corrosion current densities of under $0.1 \mu\text{A}/\text{cm}^2$ in all three, values which are maintained under constant exposure conditions.
- The addition of 2% Cl^- hinders passivation in both Portland and fly ash cement mortars, giving rise to i_{corr} values approximately 100 times higher than for chloride-free mortars.

Because corrosion penetrations $<100 \mu\text{m}$ can cause cracking and scaling in the concrete cover [24–26], the presence of chlorides would involve a drastic reduction of structures durability, a long-acknowledged shortcoming of Portland cement concrete.

In the presence of the chloride anion, i_{corr} values appear to be higher in fly ash than in Portland cement. The explanation for this behaviour may very likely lie in the way the chloride dosage was defined with respect to cement weight. Contamination is higher in the former as a result of its proportionally higher cement content, with a sand/cement ratio of 2/1, compared with a ratio of 3/1 in the latter.

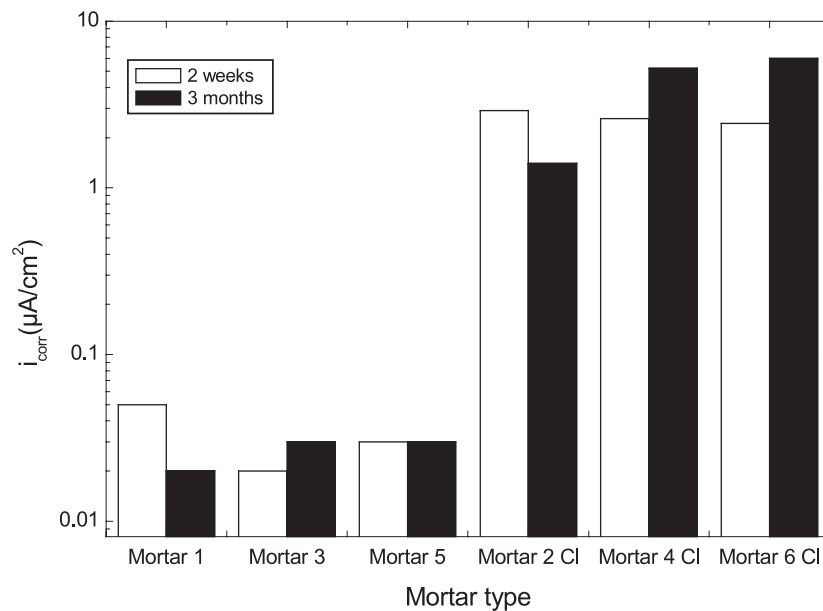


Fig. 8. Comparison of the i_{corr} a week of initiate the rehearsals and to the 3 months of exhibition, for the three types of mortar without and with (2%) of Cl^- in relation to the cement weight.

In any event, the most relevant finding is that duly manufactured, chloride-free fly ash concrete would appear to ensure reinforcing steel passivity and, concomitantly, excellent durability of reinforced concrete structures built with this new material (Figs. 3a, 4a, 5a and 8).

The E_{corr} values, in turn, are seen to be much more propitious in the absence of chlorides (Figs. 3b, 4b and 5b) and may therefore serve as an indication of reinforcement corrosion activity or passivity. Nonetheless, because this parameter provides qualitative information only and is highly dependent upon concrete moisture content, the use of (admittedly more laborious) quantitative methods in the estimation of corrosion kinetics is recommended to reliably determine the status of reinforcing steel.

4.3. Information deriving from polarisation curves and current pulses

Plotting polarisation curves calls for resorting to high polarisation values, with the inherent risk of producing irreversible effects in the electrodes, a risk that is nonetheless greatly mitigated in the steel–concrete system, where, after a recovery time of only a few hours, the i_{corr} and E_{corr} values recorded are the same as obtained prior to polarisation. The i_{corr} values deduced by intersection of the curves in Fig. 6a, b and c are similar to those obtained from the R_p measurements, providing further confirmation of the above. For a wide range of potentials, covering several hundreds of mV, the current densities corresponding to the anodic curves of the electrodes in mortars with chlorides are approximately two orders of magnitude higher than the current densities found, at the same values of electric

potential, for electrodes embedded in chloride-free mortars; these values are characteristic, respectively, of active and passive states of the steel.

The response, measured in electric potential, to a galvanostatic pulse rises by a time constant, $\tau = CR_p$, and is attenuated after the current is removed in keeping with the same time constant, as follows [27,28]:

$$\eta_t = \eta_{\text{max}} e^{-\frac{t}{CR_p}} \quad (1)$$

where: η_t is polarisation at time t ; η_{max} is the maximum polarisation reached (when current is removed) and C is double layer capacitance.

Polarisation for a time equal to τ should decline to 37% ($1/e=0.37$); consequently, this then constitutes a quick and convenient procedure for ascertaining τ and, therefore, R_p (i_{corr}), where the value of C is known.

Because C or double layer capacitance remains essentially unchanged regardless of whether the steel is in the active or passive state, with values of around $100 \mu\text{F}/\text{cm}^2$ [29], attenuation kinetics depend essentially on R_p and therefore provide a measure of corrosion rate. According to this, the faster polarisation is attenuated or the steady state prevailing prior to application of the pulse is recovered, the higher the corrosion rate. It can be readily seen from Fig. 7a, b and c that the time constants are on the order of tenths of a second or only a few seconds in chloride-contaminated mortars, whereas they reach tens of seconds in passive electrodes embedded in chloride-free mortars. Pulse shape, then, provides an instantaneous and reasonably reliable indication of reinforcement corrosion activity or passivity.

This procedure is very promising for on-site inspections. Because C is directly proportional to the area considered in

the R_p measurements and inversely proportional to R_p itself, the time constant is independent of this parameter; corrosion rates can therefore be estimated without having to know either the number or diameter of the reinforcements in the part of the structure inspected.

5. Conclusions

- Activated fly ash mortars passivate reinforcing steel as rapidly and effectively as Portland cement mortars.
- The addition of 2% (by binder weight) of Cl^- multiplies the corrosion rate by a factor of 100, approximately. In this case, the i_{corr} values are slightly higher in fly ash mortars, where the chloride content is likewise higher, due to the higher binder/sand ratio in these mortars.

References

- [1] A.K. Chatterjee, High belite cements—present status and future technological options, *Cem. Concr. Res.* 26 (1996) 1213–1225.
- [2] K.L. Scrivener, J.L. Cabiron, R. Letourneaux, High performance concrete based on calcium aluminate cements, *Cem. Concr. Res.* 29 (1999) 1215–1223.
- [3] S.A. Brooks, J.H. Sharp, Calcium aluminate cements, in: R.J. Manghabai (Ed.), *Ettringite based cements*, vol. 8(HB), E & F Spon, London, 1990, pp. 335–349.
- [4] J.H. Sharp, C.D. Lawrence, R. Yang, Calcium sulfoaluminate cement—low energy cements, *Adv. Cem. Res.* 11 (1999) 3–14.
- [5] V.D. Glukhovskiy, Soil silicates. Their properties, technology and manufacturing and fields of application. Doct Tech Sc. Degree Thesis (1965). Civil Engineering Institute. Kiev (Ukraine).
- [6] P.V. Krivenko, Alkaline cements: terminology, classification, aspects of durability, *Proc. of 10th Int. Cong. Chem. Cem.*, 1997, pp. 4iv046–4iv050. Goteborg (Sweden).
- [7] A. Palomo, M.W. Grutzeck, M.T. Blanco, Alkali-activated fly ashes. A cement for the future, *Cem. Concr. Res.* 29 (1999) 1323–1329.
- [8] J. Davidovits, Properties of geopolymer cements, in: P.V. Krivenko (Ed.), *Alkaline cements and concretes*, vol. 1, Vipol Stock, Kiev, Ukraine, 1994, pp. 131–149.
- [9] S.D. Wang, K.L. Scrivener, Hydration products of alkali activated slag cement, *Cem. Concr. Res.* 25 (1995) 561–571.
- [10] B. Tailing, J. Brandster, Present state and future of alkali-activated slag concretes, 3rd International Conference of Fly Ash, Silica Fume, Slag and Natural Pozzolans in Concrete. SP 114–74, 1989, pp. 1519–1546 Tondheim (Norway).
- [11] A. Fernández-Jiménez, A. Palomo, Activating fly ashes: enlarging the concept of cementitious material, in: R.K. Dhiri, M.D. Newlands, L.J. Csetenyi (Eds.), *International Symposia: “Role of cement science in sustainable development”*, 2003, pp. 325–334 Dundee (Scotland).
- [12] A. Palomo, A. Fernández-Jiménez, C. López-Hombrados, J.L. Lleyda, Precast elements made of alkali-activated fly ash concrete. Eighth CANMET/ACI International Conference on fly ash, silica fume, slag and natural pozzolans in concrete, Suppl. Pap. (2004) 530–545 Las Vegas, (U.S.A.).
- [13] C.L. Page, K.W.J. Treadaway, P.B. Bamforth (Eds.), *Corrosion of reinforcement in concrete*, Society of Chemical Industry, Elsevier Applied Science, London, 1990.
- [14] J.E. Slater, *Corrosion of Metals in Association With Concrete*. ASTM STP 818, 1983 Philadelphia, PA, (U.S.A.).
- [15] J. Flis, H.W. Pickering, K. Osseo-Asare, Interpretation of impedance data for reinforcing steel in alkaline solution containing chlorides and acetates, *Electrochim. Acta* 43 (1998) 1921–1929.
- [16] C. Andrade, J.A. González, Quantitative measurements of corrosion rate of reinforcing steels embedded in concrete using polarization resistance measurements, *Werk. Korros.* 29 (1978) 515–519.
- [17] J.A. González, S. Algaba, C. Andrade, Corrosion of reinforcing bars in carbonated concrete, *Br. Corros. J.* 15 (1980) 135–139.
- [18] P. Rodríguez, E. Ramírez, J.A. González, Methods for studying corrosion in reinforced concrete, *Mag. Concr. Res.* 46 (1994) 81–90.
- [19] M. Stern, A.L. Geary, Electrochemical polarization: I. A theoretical analysis of the shape of polarization curves, *J. Electrochem. Soc.* 104 (1957) 56–63.
- [20] H.F.W. Taylor, *Cement Chemistry*, Academic Press, London, 1990.
- [21] A. Palomo, S. Alonso, A. Fernández-Jiménez, I. Sobrados, J. Sanz, Alkaline activation of fly ashes. A NMR study of the reaction products, *J. Am. Ceram. Soc.* 87 (2004) 1141–1145.
- [22] A. Palomo, A. Fernández-Jiménez, M. Criado, Geopolymers: one only chemical basis, some different microstructures, *Mater. Constr.* 5 (2004) 77–91.
- [23] M. Criado, A. Fernández-Jiménez, A. Palomo, Alkali activated fly ashes. Effect of the curing procedure on the characteristics of the final product, *Fuel* (2004) (Submitted for publication).
- [24] W.D. Grimes, W.H. Hartt, D.H. Turner, Cracking of concrete in sea water due to embedded metal corrosion, *Corrosion* 35 (1979) 309–316.
- [25] C. Andrade, C. Alonso, F.J. Molina, Cover cracking as a function of bar corrosion: Part I. Experimental test, *Mater. Struct.* 26 (1993) 453–464.
- [26] J.A. González, S. Feliu, P. Rodríguez, Threshold steel corrosion rates for durability problems in reinforced structures, *Corrosion* 53 (1997) 65–71.
- [27] G.K. Glass, An assessment of the coulometric method applied to the corrosion of steel in concrete, *Corros. Sci.* 35 (1995) 597–605.
- [28] J.A. González, A. Cobo, M.N. González, S. Feliu, On-site determination of corrosion rate in reinforced concrete structures by use of galvanostatic pulses, *Corros. Sci.* 43 (2001) 611–625.
- [29] P. Rodríguez, J.A. González, Use of the coulometric method for measuring corrosion rates of embedded metal in concrete, *Mag. Concr. Res.* 46 (1994) 91–97.